



**HAL**  
open science

# Exponential Adams Bashforth integrators for stiff ODEs, application to cardiac electrophysiology

Yves Coudière, Charlie Douanla Lontsi, Charles Pierre

## ► To cite this version:

Yves Coudière, Charlie Douanla Lontsi, Charles Pierre. Exponential Adams Bashforth integrators for stiff ODEs, application to cardiac electrophysiology. 2017. hal-01394036v3

**HAL Id: hal-01394036**

**<https://hal.science/hal-01394036v3>**

Preprint submitted on 20 Sep 2017 (v3), last revised 25 Apr 2018 (v4)

**HAL** is a multi-disciplinary open access archive for the deposit and dissemination of scientific research documents, whether they are published or not. The documents may come from teaching and research institutions in France or abroad, or from public or private research centers.

L'archive ouverte pluridisciplinaire **HAL**, est destinée au dépôt et à la diffusion de documents scientifiques de niveau recherche, publiés ou non, émanant des établissements d'enseignement et de recherche français ou étrangers, des laboratoires publics ou privés.

# Exponential Adams Bashforth integrators for stiff ODEs, application to cardiac electrophysiology

Yves Coudière<sup>a,b,c</sup>, Charlie Douanla Lontsi<sup>a,c,b</sup>, Charles Pierre<sup>d</sup>

<sup>a</sup>IHU Liryc, Electrophysiology and Heart Modeling, 33600 Pessac, France

<sup>b</sup>IMB, UMR 5251 CNRS, Université de Bordeaux, Bordeaux-INP, 33400 Talence, France

<sup>c</sup>Carmen team, Inria Bordeaux Sud-Ouest, 33400 Talence, France

<sup>d</sup>LMAP, UMR 5142 CNRS, Université de Pau, 64000 Pau, France

---

## Abstract

Models in cardiac electrophysiology are coupled systems of reaction diffusion PDE and of ODE. The ODE system displays a very stiff behavior. It is non linear and its upgrade at each time step is a preponderant load in the computational cost. The issue is to develop high order explicit and stable methods to cope with this situation.

In this article, is is analyzed the resort to exponential Adams Bashforth (EAB) integrators in cardiac electrophysiology. The method is presented in the framework of a general and varying stabilizer, that is well suited in this context. Stability under perturbation (or 0-stability) is proven. It provides a new approach for the convergence analysis of the method. The Dahlquist stability properties of the method is performed. It is presented in a new framework that incorporates the discrepancy between the stabilizer and the system Jacobian matrix. Provided this discrepancy is small enough, the method is shown to be A(alpha)-stable. This result is interesting for an explicit time-stepping method. Numerical experiments are presented for two classes of stiff models in cardiac electrophysiology. They include performances comparisons with several classical methods. The EAB method is observed to be as stable as implicit solvers and cheaper at equal level of accuracy.

*Keywords:* stiff equations, explicit high-order multistep methods, exponential integrators of Adams type, stability and convergence, Dahlquist stability

*2000 MSC:* 65L04, 65L99, 65L06, 65L20

---

## 1. Introduction

Computations in cardiac electrophysiology have to face two constraints. Firstly the stiffness due to heterogeneous time and space scales. This is usually dealt with by considering very fine grids. This strategy is associated with large computational costs, still challenging in dimension three. Secondly, the resolution of the reaction terms from the ionic models has an important cost. This resolution occur at each grid node. The total amount of evaluation of the reaction terms has to be maintained as low as possible. For this reason, implicit solvers are usually avoided.

---

\*Inria, 200 Avenue Vieille Tour, 33400 Talence, France

Email address: [yves.coudiere@u-bordeaux.fr](mailto:yves.coudiere@u-bordeaux.fr) (Yves Coudière)

Exponential integrators are well adapted to cope with these two constraints. Actually they allow an explicit resolution of the reaction term, and display strong stability properties. In this article, we study and analyze exponential time-stepping methods dedicated to the resolution of reaction equations.

Models for the propagation of the cardiac action potential are evolution reaction diffusion equations coupled with ODE systems. The widely used monodomain model [1, 2, 3] formulates as  $\frac{\partial v}{\partial t} = Av + f_1(v, w, x, t)$  and  $\frac{\partial w}{\partial t} = f_2(v, w, x, t)$ , with space and time variables  $x \in \Omega \subset \mathbb{R}^d$  and  $t \in \mathbb{R}$ . The unknowns are the functions  $v(t, x) \in \mathbb{R}$  (the transmembrane voltage) and  $w(t, x) \in \mathbb{R}^N$  (a vector that gathers variables describing pointwise the electrophysiological state of the heart cells). In the monodomain model, the diffusion operator is  $A(:= \text{div}(g(x)\nabla\cdot))$ , and the reaction terms are the nonlinear functions  $f_1, f_2$ . These functions model the cellular electrophysiology. They are called ionic models. Ionic models are of complex nature, see e.g. [4, 5, 6, 7]. A special attention has to be paid to the number of evaluations of the functions  $f_1$  and  $f_2$ , and implicit solvers are usually avoided. Though we ultimately use an implicit/explicit method to solve the PDE, we need an efficient, fast and robust method to integrate the reaction terms. Therefore, this article focuses on the time integration of the stiff ODE system

$$\frac{dy}{dt} = f(t, y), \quad y(0) = y_0, \quad (1)$$

in the special cases where  $f(t, y)$  is an ionic model from cellular electrophysiology. In this case, stiffness is due to the co-existence of fast and slow variables. Fast variables are given in (1) by equations of the form,

$$\frac{dy_i}{dt} = f_i(t, y) = a_i(t, y)y_i + b_i(t, y). \quad (2)$$

Here  $a_i(t, y) \in \mathbb{R}$  is provided by the model. This scalar rate of variation will be inserted in the numerical method to stabilize its resolution.

Exponential integrators are a class of explicit methods meanwhile exhibiting strong stability properties. They have motivated many studies along the past 15 years, among which we quote e.g. [8, 9, 10, 11, 12, 13] and refer to [14, 15, 16] for general reviews. They have already been used in cardiac electrophysiology, as e.g. in [17, 18]. Exponential integrators are based on a reformulation of (1) as,

$$\frac{dy}{dt} = a(t, y)y + b(t, y), \quad y(0) = y_0, \quad (3)$$

(with  $f = ay + b$ ) where the linear part  $a(t, y)$  is used to stabilize the resolution. Basically  $a(t, y)$  is assumed to capture the stiffest modes of the Jacobian matrix of system (1). Stabilization is brought by performing an exact integration of these modes. This exact integration involves the computation of the exponential  $\exp(a(t_n, y_n)h)$  at the considered point. This computation is the supplementary cost for exponential integrators as compared to other time stepping methods.

Exponential integrators of Adams type are explicit multistep exponential integrators. They were first introduced by Certaine [19] in 1960 and Nørsett [20] in 1969 for a constant linear part  $A = a(t, y)$  in (3). The schemes are derived using a polynomial interpolation of the non linear term  $b(t, y)$ . It recently received an increasing interest [21, 22, 23] and various convergence analysis have been completed in this particular case [24, 25, 26]. Non constant linear parts have been less studied. Lee and Preiser [27] in 1978 and by Chu [28] in 1983 first suggested to rewrite the equation (1) at each time instant  $t_n$  as, rewritten as,

$$\frac{dy}{dt} = a_n y + g_n(t, y), \quad y(t_n) = y_n, \quad (4)$$

with  $a_n = a(t_n, y_n)$  and  $g_n(t, y) = b(t, y) + (a(t, y) - a_n)y$ . In the sequel,  $a_n$  is referred to as the *stabilizer*. It is updated after each time step. Recently, Ostermann *et al* [24, 26] analyzed the linearized exponential Adams method, where the stabilizer  $a_n$  is set to the Jacobian matrix of  $f(t, y)$  in (1). This choice requires the computation of a matrix exponential at every time step. Anyway, when the fast variables of the system are known, stabilization can be performed only on these variables. Considering the full Jacobian as the stabilizer implies unnecessary computational efforts. To avoid these problems, an alternative is to set the stabilizer as a part or as an approximation of the Jacobian. This has been analyzed in [29] and in [30] for exponential Rosenbrock and exponential Runge Kutta type methods respectively. This strategy is well adapted to cardiac electrophysiology, where a diagonal stabilizer associated with the fast variables is directly provided by the model with equation (2). The present contribution is to analyze general varying  $a(t, y)$  in (3) for exponential integrators of Adams type, referred to as *exponential Adams Bashforth*, and shortly denoted EAB. Together with the EAB scheme, we introduce a new variant, that we called *integral exponential Adams Bashforth*, denoted I-EAB.

The convergence analysis held in [24] extends to the case of general varying stabilizers. However there is a lack of results concerning the stability in this case: for instance, consider the simpler exponential Euler method, defined by  $y_{n+1} = s(t_n, y_n, h) := e^{a_n h} y_n + h\varphi_1(a_n h)b_n$  with  $\varphi_1(z) = (e^z - 1)/z$ . Stability under perturbation (also called 0-stability) can be easily proven provided that the scheme generator  $s(t, y, h)$  is globally Lipschitz in  $y$  with a constant bounded by  $1 + Ch$ . Therefore stability under perturbation is classically studied by analyzing the partial derivative  $\partial_y s$ . This can be done in the case where  $a(t, y)$  is either a constant operator or a diagonal varying matrix. In the general case however things turn out to be more complicated. Indeed the general expansion  $e^{M+\varepsilon N} \neq e^M + \varepsilon e^M N + O(\varepsilon^2)$  does not hold, unless the two matrices  $M$  and  $N$  are commuting. *As a consequence differentiating  $e^{a(t,y)h}$  in  $y$  cannot be done without very restrictive assumptions on  $a(t, y)$ .* We present here a stability analysis for general varying stabilizers. This will be done by introducing relaxed stability conditions on the scheme generator  $s(t, y, h)$ . Together with a consistency analysis, it provides a new proof for the convergence of the EAB schemes, in the spirit of [24].

Stability under perturbation provides results of qualitative nature. In addition, the Dahlquist stability analysis strengthens these results. It is a practical tool that allows to dimension the time step  $h$  with respect to the variations of  $f(t, y)$  in equation (1). The analysis is made by setting  $f(t, y) = \lambda y$  in (1). For exponential integrators with general varying stabilizer, the analysis must incorporate the decomposition of  $f(t, y) = \lambda y$  used in (3). The stability domain of the considered method will depend on the relationship between  $\lambda$  and  $a(t, y)$ , following a concept first introduced in [17]. We numerically establish that EAB methods are  $A(\alpha)$  stable provided that the stabilizer is sufficiently close to the system Jacobian matrix (precise definitions are in section 5). Moreover the angle  $\alpha$  approaches  $\pi/2$  when the stabilizer goes to the system Jacobian matrix. In contrast, there exists no  $A(0)$  stable explicit linear multistep method (see [31, chapter V.2]). This property is remarkable for explicit methods.

Numerical experiments for the EAB and I-EAB scheme are provided in section 6, in the context of cardiac electrophysiology. Robustness to stiffness is studied with this choice. It is numerically shown to be comparable to implicit methods both in terms of accuracy and of stability condition on the time step. We conclude that EAB methods are well suited for solving stiff differential problems. In particular they allow computations at large time step with good accuracy properties and cheap cost.

The article is organized as follows. The EAB and I-EAB methods are introduced in section 2. The general stability and convergence results are stated and proved in section 3. The EAB and

I-EAB stability under perturbation and convergence are proved in section 4. The Dahlquist stability is investigated in section 5, and the numerical experiments end the article, in section 6.

In all this paper,  $h > 0$  is a constant time-step and  $t_n = nh$  are the time instants associated with the numerical approximate  $y_n$  of the solution of the ODE (1).

## 2. Scheme definitions

### 2.1. The EAB<sub>k</sub> method

The exact solution at time  $t_{n+1}$  to the equation (4) (with  $a_n = a(t_n, y_n)$ ) is given by the variation of the constants formula

$$y(t_{n+1}) = e^{a_n h} \left( y(t_n) + \int_0^h e^{-a_n \tau} g_n(t_n + \tau, y(t_n + \tau)) d\tau \right). \quad (5)$$

Using the  $k$  approximations  $y_{n-j} \simeq y(t_{n-j})$  for  $j = 0 \dots k-1$ , we build the Lagrange polynomial  $\tilde{g}_n$  of degree at most  $k-1$  that satisfies,

$$\tilde{g}_n(t_{n-j}) = g_{nj} := g(t_{n-j}, y_{n-j}), \quad 0 \leq j \leq k-1. \quad (6)$$

It provides the numerical approximation  $y_{n+1} \simeq y(t_{n+1})$  as

$$y_{n+1} = e^{a_n h} \left( y_n + \int_0^h e^{-a_n \tau} \tilde{g}_n(t_n + \tau) d\tau \right). \quad (7)$$

The Taylor expansion of the polynomial  $\tilde{g}_n$  is  $\tilde{g}_n(t_n + \tau) = \sum_{j=1}^k \frac{\gamma_{nj}}{(j-1)!} (\tau/h)^{j-1}$ , where the coefficients  $\gamma_{nj}$  are uniquely determined by (6), and actually given in table 1 for  $k = 1, 2, 3, 4$ . An exact integration of the integral in equation (7) may be performed:

$$y_{n+1} = e^{a_n h} y_n + h \sum_{j=1}^k \varphi_j(a_n h) \gamma_{nj}, \quad (8)$$

where the functions  $\varphi_j$ , originally introduced in [20], are recursively defined (for  $j \geq 0$ ) by,

$$\varphi_0(z) = e^z, \quad \varphi_{j+1}(z) = \frac{\varphi_j(z) - \varphi_j(0)}{z} \quad \text{and} \quad \varphi_j(0) = \frac{1}{j!}. \quad (9)$$

The equation (8) defines the Exponential Adams Bashforth method of order  $k$ , denoted by EAB<sub>k</sub>.

Table 1: Coefficients  $\gamma_{nj}$  for the EAB<sub>k</sub> schemes

$k$	1	2	3	4
$\gamma_{n1}$	$g_n$	$g_n$	$g_n$	$g_n$
$\gamma_{n2}$		$g_n - g_{n-1}$	$\frac{3}{2}g_n - 2g_{n-1} + \frac{1}{2}g_{n-2}$	$\frac{11}{6}g_n - 3g_{n-1} + \frac{3}{2}g_{n-2} - \frac{1}{3}g_{n-3}$
$\gamma_{n3}$			$g_n - 2g_{n-1} + g_{n-2}$	$2g_n - 5g_{n-1} + 4g_{n-2} - g_{n-3}$
$\gamma_{n4}$				$g_n - 3g_{n-1} + 3g_{n-2} - g_{n-3}$

*Remark 1.* When  $a(t, y) = \text{diag}(d_i)$  is a diagonal matrix,  $\varphi_k(a_n h) = \text{diag}(\varphi_k(d_i))$  can be computed component-wise. Its computation is straightforward.

*Remark 2.* With the definition (9), the functions  $\varphi_k$  are analytic on the whole complex plane. Therefore the  $\text{EAB}_k$  scheme definition (8) makes sense for a matrix term  $a(t, y)$  in equation (3) without particular assumption.

*Remark 3.* The computation of  $y_{n+1}$  in the formula (8) requires the computation of  $\varphi_j(a_n h)$  for  $j = 0, \dots, k$ . This computational effort can be reduced with the recursive definition (9). In practice only  $\varphi_0(a_n h)$  needs to be computed. This is detailed in section 6.1.

## 2.2. A variant: the I-EAB<sub>k</sub> method

If the matrix  $a(t, y)$  is diagonal, we can take advantage of the following version for the variation of the constants formula

$$y(t_{n+1}) = e^{A_n(h)} \left( y(t_n) + \int_0^h e^{-A_n(\tau)} b(y(t_n + \tau), t_n + \tau) d\tau \right),$$

where  $A_n(\tau) = \int_0^\tau a(t_n + \sigma, y(t_n + \sigma)) d\sigma$ . An attempt to improve the  $\text{EAB}_k$  formula (8) is to replace  $a(t, y)$  and  $b(t, y)$  in the integral above by their Lagrange interpolation polynomials. At time  $t_n$ , we define the two polynomials  $\tilde{a}_n$  and  $\tilde{b}_n$  of degree at most  $k - 1$  so that  $\tilde{a}_n(t_{n-j}) = a(t_{n-j}, y_{n-j})$ , and  $\tilde{b}_n(t_{n-j}) = b(t_{n-j}, y_{n-j})$ , for  $j = 0 \dots k - 1$ , and the primitive  $\tilde{A}_n(\tau) = \int_0^\tau \tilde{a}_n(t_n + \sigma, y(t_n + \sigma)) d\sigma$ . The resulting approximate solution at time  $t_{n+1}$  is finally given by the formula

$$y_{n+1} = e^{\tilde{A}_n(h)} \left( y_n + \int_0^h e^{-\tilde{A}_n(\tau)} \tilde{b}_n(t_n + \tau) d\tau \right). \quad (10)$$

The method is denoted I-EAB<sub>k</sub>, for integral EAB<sub>k</sub>. Unlike for the formula (7), no exact integration formula is available, because of the term  $e^{-\tilde{A}_n(\tau)}$ . A quadrature rule is required for the actual numerical computation of the integral in formula (10). Implementation details are given in section 6.1.

## 3. Stability conditions and convergence

The equation (1) is considered on a finite dimensional vector space  $E$  with norm  $|\cdot|_E$ . We fix a final time  $T > 0$  and assume that equation (1) has a solution  $y$  on  $[0, T]$ . We adopt the general settings for the analysis of  $k$ -multistep methods following [32]. The space  $E^k$  is equipped with the maximum norm  $|Y|_\infty = \max_{1 \leq i \leq k} |y_i|_E$  with  $Y = (y_1, \dots, y_k) \in E^k$ . A  $k$ -multistep scheme is defined by a mapping  $s : (t, Y, h) \in \mathbb{R} \times E^k \times \mathbb{R}^+ \mapsto s(t, Y, h) \in E$ . For instance, the  $\text{EAB}_k$  scheme rewrites with  $Y = (y_{n-k+1}, \dots, y_n)$  in the formula (8), and  $s(t_n, Y, h) = y_{n+1}$ . The scheme generator is the mapping  $S$  given by  $S : (t, Y, h) \in \mathbb{R} \times E^k \times \mathbb{R}^+ \mapsto (y_2, \dots, y_k s(t, Y, h)) \in E^k$ . A numerical solution is a sequence  $(Y_n)$  in  $E^k$  for  $n \geq k - 1$  so that

$$Y_{n+1} = S(t_n, Y_n, h) \quad \text{for } n \geq k - 1, \quad (11)$$

and  $Y_{k-1} = (y_0, \dots, y_{k-1})$  is a given initial data. A perturbed numerical solution is a sequence  $(Z_n)$  in  $E^k$  for  $n \geq k - 1$  such that,

$$Z_{k-1} = Y_{k-1} + \xi_{k-1}, \quad Z_{n+1} = S(t_n, Z_n, h) + \xi_{n+1} \quad \text{for } n \geq k - 1, \quad (12)$$

with  $(\xi_n) \in E^k$  for  $n \geq k - 1$ . The scheme is said to be stable under perturbation (or 0-stable) if, for any numerical solution  $(Y_n)$  as in (11), there exists a (stability) constant  $L_s > 0$  such that, for any perturbation  $(Z_n)$  as defined in (12), we have,

$$\max_{k-1 \leq n \leq T/h} |Y_n - Z_n|_\infty \leq L_s \sum_{k-1 \leq n \leq T/h} |\xi_n|_\infty. \quad (13)$$

**Proposition 1.** Assume that there exists constants  $C_1 > 0$  and  $C_2 > 0$  such that,

$$1 + |S(t, Y, h)|_\infty \leq (1 + |Y|_\infty)(1 + C_1 h), \quad (14)$$

$$|S(t, Y, h) - S(t, Z, h)|_\infty \leq |Y - Z|_\infty (1 + C_2 h(1 + |Y|_\infty)), \quad (15)$$

for  $0 \leq t \leq T$ , and for  $Y, Z \in E^k$ . Then, the numerical scheme is stable under perturbation with the constant  $L_s$  in (13) given by,

$$L_s = e^{C^* T}, \quad C^* := C_2 e^{C_1 T} (1 + |Y_{k-1}|_\infty). \quad (16)$$

*Proof.* Consider a numerical solution  $(Y_n)$  in (11). A recursion on condition (14) gives,

$$1 + |Y_n|_\infty \leq (1 + |Y_{k-1}|_\infty)(1 + C_1 h)^{n-k+1} \leq e^{C_1 T} (1 + |Y_{k-1}|_\infty),$$

since  $(1 + x)^p \leq e^{px}$  (for  $x \geq 0$ ), and  $(n - k + 1)h \leq nh \leq T$ . Now, consider a perturbation  $(Z_n)$  of  $(Y_n)$  given by (12). Using the condition (15) together with the previous inequality,

$$\begin{aligned} |Y_{n+1} - Z_{n+1}|_\infty &\leq |S(t_n, Y_n, h) - S(t_n, Z_n, h)|_\infty + |\xi_{n+1}|_\infty \leq |Y_n - Z_n|_\infty (1 + C_2 h(1 + |Y_n|_\infty)) + |\xi_{n+1}|_\infty \\ &\leq |Y_n - Z_n|_\infty (1 + C_2 e^{C_1 T} (1 + |Y_{k-1}|_\infty) h) + |\xi_{n+1}|_\infty \leq |Y_n - Z_n|_\infty (1 + C^* h) + |\xi_{n+1}|_\infty, \end{aligned}$$

where  $C^* := C_2 e^{C_1 T} (1 + |Y_{k-1}|_\infty)$ . By recursion we get,

$$\begin{aligned} |Y_n - Z_n|_\infty &\leq (1 + C^* h)^{n-k+1} |Y_{k-1} - Z_{k-1}|_\infty + \sum_{i=0}^{n-k} (1 + C^* h)^i |\xi_{n-i}|_\infty \\ &\leq (1 + C^* h)^n \sum_{i=k-1}^n |\xi_i|_\infty \leq e^{C^* T} \sum_{i=k-1}^n |\xi_i|_\infty, \end{aligned}$$

which ends the proof.  $\square$

Like in the classical cases, stability under perturbation together with consistency ensures convergence. Let us specify this point. For the considered solution  $y(t)$  of problem (1) on  $[0, T]$ , we define,

$$Y(t) = (y(t - (k - 1)h), \dots, y(t)) \in E^k \quad \text{for } 0 \leq (k - 1)h \leq t \leq T. \quad (17)$$

The local error at time  $t_n$  is,

$$\varepsilon(t_n, h) = Y(t_{n+1}) - S(t_n, Y(t_n), h). \quad (18)$$

The scheme is said to be consistent of order  $p$  if there exists a (consistency) constant  $L_c > 0$  only depending on  $y(t)$  such that,  $\max_{k-1 \leq n \leq T/h} |\varepsilon(t_n, h)|_\infty \leq L_c h^{p+1}$ .

**Corollary 1.** *If the scheme satisfies the stability conditions (14) and (15), and is consistent of order  $p$ , then a numerical solution  $(Y_n)$  given by (11) satisfies,*

$$\max_{k-1 \leq n \leq T/h} |Y(t_n) - Y_n|_\infty \leq L_s L_c T h^p + L_s |\xi_0|_\infty, \quad (19)$$

where  $\xi_0 = Y(t_{k-1}) - Y_{k-1}$  denotes the error on the initial data, and the constant  $L_s$  is as in equation (16).

*Remark 4.* Note that the stability constant  $L_s$  in (16) depends on  $|Y_{k-1}|_\infty$ , and then on  $h$ . This is not a problem since  $L_s$  can be bounded uniformly as  $h \rightarrow 0$  for  $Y_{k-1}$  in a neighborhood of  $y_0$ .

*Proof.* We have  $Y(t_{k-1}) = Y_{k-1} + \xi_0$  and  $Y(t_{n+1}) = S(t_n, Y(t_n), h) + \varepsilon(t_n, h)$ . Therefore the sequence  $(Y(t_n))$  is a perturbation of the numerical solution  $(Y_n)$  in the sense of (12). As a consequence, proposition 1 shows that

$$\max_{k-1 \leq n \leq T/h} |Y_n - Y(t_n)|_E \leq L_s \left( |\xi_0| + \sum_{k \leq n \leq T/h} |\varepsilon(t_n, h)| \right) \leq L_s |\xi_0| + L_s L_c \left( \sum_{k \leq n \leq T/h} h \right) h^p,$$

and the convergence result follows.  $\square$

#### 4. EAB<sub>k</sub> and I-EAB<sub>k</sub> scheme analysis

The space  $E$  is assumed to be  $E = \mathbb{R}^N$  with its canonical basis and with  $|\cdot|_E$  the maximum norm. The space of operators on  $E$  is equipped with the associated operator norm, and associated to  $N \times N$  matrices. Thus  $a(t, y)$  is a  $N \times N$  matrix and its norm  $|a(t, y)|$  is the matrix norm associated to the maximum norm on  $\mathbb{R}^N$ .

It is commonly assumed for the numerical analysis of ODE solvers that  $f$  in the equation (1) is uniformly Lipschitz in its second component  $y$ . With the formulation (3), the following assumptions will be needed: on  $\mathbb{R} \times E$ ,

$$|a(t, y)| \leq M_a, \quad a(t, y), \quad b(t, y) \quad \text{and} \quad f(t, y) \quad \text{uniformly Lipschitz in } y. \quad (20)$$

We denote by  $K_f$ ,  $K_a$  and  $K_b$  the Lipschitz constant for  $f$ ,  $a$  and  $b$  respectively.

**Theorem 1.** *With the assumptions (20), the EAB<sub>k</sub> and I-EAB<sub>k</sub> schemes are stable under perturbations. Moreover, if  $a$  and  $b$  are  $C^k$  regular on  $\mathbb{R} \times E$ , then the EAB<sub>k</sub> and I-EAB<sub>k</sub> schemes are consistent of order  $k$ . Therefore they converge with order  $k$  in the sense of inequality (19), by applying corollary 1.*

The stability and consistency are proved in sections 4.3 and 4.4, respectively. Preliminary tools and definitions are provided in the sections 4.1 and 4.2.

##### 4.1. Interpolation results

Consider a function  $x : \mathbb{R} \times E \rightarrow \mathbb{R}$  and a triplet  $(t, Y, h) \in \mathbb{R} \times E^k \times \mathbb{R}^+$  with  $Y = (y_1, \dots, y_k)$ . We set to  $\tilde{x}_{[t, Y, h]}$  the polynomial with degree at most  $k - 1$  so that

$$\tilde{x}_{[t, Y, h]}(t - ih) = x(t - ih, y_{k-i}), \quad 0 \leq i \leq k - 1.$$

We then extend component-wise this definition to vector valued or matrix valued functions  $x$  (e.g. the functions  $a$  or  $b$ ).



**Lemma 1.** *There exists an (interpolation) constant  $L_i > 0$  such that, for any function  $x : \mathbb{R} \times E \mapsto \mathbb{R}$ , and for any vectors  $Y, Z \in E^k$ ,*

$$\sup_{t \leq \tau \leq t+h} |\tilde{x}_{[t, Y, h]}(\tau)| \leq L_i \max_{0 \leq i \leq k-1} |x(t - ih, y_{k-i})|, \quad (21)$$

$$\sup_{t \leq \tau \leq t+h} |\tilde{x}_{[t, Y, h]}(\tau) - \tilde{x}_{[t, Z, h]}(\tau)| \leq L_i \max_{0 \leq i \leq k-1} |x(t - ih, y_{k-i}) - x(t - ih, z_{k-i})|. \quad (22)$$

Consider a function  $y : [0, T] \rightarrow E$  and assume that  $x$  and  $y$  have a  $C^k$  regularity. Then, when  $[t - (k-1)h, t+h] \subset [0, T]$ ,

$$\sup_{t \leq \tau \leq t+h} |x(\tau, y(\tau)) - \tilde{x}_{[t, Y(t), h]}(\tau)|_E \leq \sup_{[0, T]} \left| \frac{d^k}{dt^k} (f(t, y(t))) \right| h^k, \quad (23)$$

with  $Y(t)$  defined in (17).

For a vector valued function in  $\mathbb{R}^d$  the previous inequalities hold when considering the max norm on  $\mathbb{R}^d$ . For a matrix valued function in  $\mathbb{R}^d \times \mathbb{R}^d$  this is also true for the operator norm on  $\mathbb{R}^d \times \mathbb{R}^d$  when multiplying the constants in the inequalities (21), (22) and (23) by  $d$ .

*Proof.* The space  $\mathbb{P}_{k-1}$  of the polynomials  $p$  with degree at most  $k-1$  is equipped with the norm  $\sup_{[0,1]} |p(\tau)|$ . We associate to the  $R = (r_1, \dots, r_k) \in \mathbb{R}^k$  its Lagrange interpolation polynomial  $\mathcal{L}R \in \mathbb{P}_{k-1}$ , uniquely determined by  $\mathcal{L}R(-i) = r_{k-i}$  for  $i = 0 \dots k-1$ . The mapping  $\mathcal{L}$  is linear. Let  $C_{\mathcal{L}}$  be its continuity constant (it only depends on  $k$ ).

We fix the function  $x : \mathbb{R} \times E \rightarrow \mathbb{R}$  and  $(t, h) \in \mathbb{R} \times \mathbb{R}^+$ . Consider the vector  $Y = (y_1, \dots, y_k) \in E^k$  and define the vector  $R = (x(t - (k-1)h, y_1), \dots, x(t, y_k)) \in \mathbb{R}^k$ . We have  $\tilde{x}_{[t, Y, h]}(t + \tau) = \mathcal{L}R(\tau/h)$ . The relation (21) is exactly the continuity of  $\mathcal{L}$  and  $L_i = C_{\mathcal{L}}$ .

Consider  $Y_1, Y_2 \in E^k$  and the associated vectors  $R_1, R_2$  as above. We have  $(x_{[t, Y_1, h]} - x_{[t, Y_2, h]})(t + \tau) = \mathcal{L}(R_1 - R_2)(\tau/h)$ . Again, relation (22) is derived from the continuity of  $\mathcal{L}$ .

Let  $\varphi : \mathbb{R} \rightarrow \mathbb{R}$  be a  $C^k$  function, its interpolation polynomial  $\tilde{\varphi}$  at the points  $t - (k-1)h, \dots, t$  is considered. A classical result on Lagrange interpolation applied to  $\varphi$  states that, for all  $\tau \in (t, t+h)$ , there exists  $\xi \in (t - (k-1)h, t+h)$ , such that  $(\varphi - \tilde{\varphi})(\tau) = \frac{1}{k!} \varphi^{(k)}(\xi) \pi(\tau)$ , where  $\pi(\tau) = \prod_{i=1}^k (\tau - t_i)$ . For  $\tau \in (t, t+h)$ , we have  $|\pi(\tau)| \leq k! h^k$ . This proves (23) by setting  $\varphi(t) = x(t, y(t))$ .

For a vector valued function  $x : \mathbb{R} \times E \rightarrow \mathbb{R}^d$ , these three inequalities holds by processing component-wise and when considering the max norm on  $\mathbb{R}^d$ .

For a matrix valued function  $x : \mathbb{R} \times E \rightarrow \mathbb{R}^d \times \mathbb{R}^d$ , the extension is direct when considering the max norm  $|\cdot|_{\infty}$  on  $\mathbb{R}^d \times \mathbb{R}^d$  (i.e. the max norm on the matrix entries). The operator norm  $|\cdot|$  is retrieved with the inequality  $|\cdot|_{\infty} \leq d|\cdot|$ .  $\square$

#### 4.2. Scheme generators

Let us consider  $(t, Y, h) \in \mathbb{R} \times E^k \times \mathbb{R}^+$  with  $Y = (y_1, \dots, y_k)$ . With the notations used in the previous subsection, we introduce the interpolations  $\tilde{a}_{[t, Y, h]}$  and  $\tilde{b}_{[t, Y, h]}$  for the functions  $a$  and  $b$  (in (3)). Thanks to its definition (10), the I-EAB $_k$  scheme generator is defined by,

$$s(t, Y, h) = z(t+h) \quad \text{with} \quad \frac{dz}{d\tau} = \tilde{a}_{[t, Y, h]}(\tau)z(\tau) + \tilde{b}_{[t, Y, h]}(\tau), \quad z(t) = y_k. \quad (24)$$

We introduce the polynomial  $\bar{g}_{[t, Y, h]}$  with degree at most  $k-1$  that satisfies,

$$\bar{g}_{[t, Y, h]}(t - ih) = f(t - ih, y_{k-i}) - a(t, y_k)y_{k-i}, \quad i = 0 \dots k-1.$$

The function  $\tilde{g}_n$  in (6) is given by  $\tilde{g}_n = \bar{g}_{[t_n, Y_n, h]}$  with  $Y_n = (y_{n-k+1}, \dots, y_n)$ . With the definition (7), the EAB $_k$  scheme generator is defined by,

$$s(t, Y, h) = z(t+h) \quad \text{with} \quad \frac{dz}{dt} = a(t, y_k)z(\tau) + \bar{g}_{[t, Y, h]}(\tau), \quad z(t) = y_k. \quad (25)$$

We will use the fact that  $\bar{g}_{[t, Y, h]}$  is the Lagrange interpolation polynomial of the function  $g_{t, y_k} : (\tau, \xi) \mapsto f(\tau, \xi) - a(t, y_k)\xi$ .

These scheme generator definitions will allow us to use the following Gronwall's inequality (see [33, Lemma 196, p.150]).

**Lemma 2.** *Suppose that  $z(t)$  is a  $C^1$  function on  $E$ . If there exist  $\alpha > 0$  and  $\beta > 0$  such that  $|z'(t)|_E \leq \alpha t + \beta$  for all  $t \in [t_0, t_0 + h]$ , then:*

$$|z(t)|_E \leq |z(t_0)|_E e^{\alpha h} + \beta h e^{\alpha h} \quad \text{for } t \in [t_0, t_0 + h]. \quad (26)$$

### 4.3. Stability

According to proposition 1, we have to prove the stability conditions (14) and (15). It is sufficient to prove these relations for  $h \leq h_0$  for some constant  $h_0 > 0$  since the limit  $h \rightarrow 0$  is of interest here.

#### 4.3.1. Case of the I-EAB $_k$ scheme

Consider  $(t, h) \in \mathbb{R} \times \mathbb{R}^+$  and  $Y = (y_1, \dots, y_k) \in E^k$ . We simply denote  $\tilde{a} = \tilde{a}_{[t, Y, h]}$  and  $\tilde{b} = \tilde{b}_{[t, Y, h]}$ . The scheme generator is given by (24). We first have to bound  $z(t+h)$  where  $z$  is given by,  $z' = \tilde{a}z + \tilde{b}$ , and  $z(t) = y_k$ . Firstly, with the interpolation bound (21),  $\sup_{t \leq \tau \leq t+h} |\tilde{a}(\tau)| \leq L_i \max_{0 \leq i \leq k-1} |a(t-ih, y_{k-i})| \leq L_i M_a := \alpha$ . Secondly, the function  $b(t, y)$  is globally Lipschitz in  $y$  and thus can be bounded by  $|b(t, y)|_E \leq |b(t, 0)|_E + K_b |y|_E \leq R_b(|y|_E + 1)$ , for  $0 \leq t \leq T$  and for some constant  $R_b$  only depending on  $K_b$  and on  $T$ . Then with the bound (21),  $\sup_{t \leq \tau \leq t+h} |\tilde{b}(\tau)|_E \leq L_i \max_{0 \leq i \leq k-1} R_b (|y_{k-i}|_E + 1) \leq L_i R_b (|Y|_\infty + 1) := \beta$ . By applying the Gronwall inequality (26) with these  $\alpha$  and  $\beta$ , for  $0 \leq \tau \leq h$ ,  $|z(t+\tau)|_E \leq e^{L_i M_a \tau} (|y_k|_E + h L_i R_b (|Y|_\infty + 1))$ . Thus, there exists a constant  $C_1$  only depending on  $L_i, M_a, R_b$  and  $h_0$  such that, for  $0 \leq \tau \leq h$  and  $0 \leq h \leq h_0$ ,

$$|z(t+\tau)|_E \leq C_1 h + |Y|_\infty (1 + C_1 h). \quad (27)$$

This gives the condition (14), by taking  $\tau = h$ .

For  $j=1, 2$  We consider  $Y_j = (y_{j,1}, \dots, y_{j,k}) \in E^k$  and denote  $\tilde{a}_j = \tilde{a}_{[t, Y_j, h]}$  and  $\tilde{b}_j = \tilde{b}_{[t, Y_j, h]}$  the interpolations of the functions  $a$  and  $b$ . With the definition (24) of the I-EAB $_k$  scheme, we have  $|s(t, Y_1, h) - s(t, Y_2, h)|_E = |\delta(t+h)|$  with  $\delta = z_1 - z_2$  and with  $z_j$  given by  $z'_j = \tilde{a}_j z_j + \tilde{b}_j$ , and  $z_j(t) = y_{j,k}$ . We have then  $\delta' = \tilde{a}_1 \delta + r$ , and  $r := (\tilde{a}_1 - \tilde{a}_2)z_2 + (\tilde{b}_1 - \tilde{b}_2)$ . Using that  $a$  and  $b$  are Lipschitz in  $y$  and with the interpolation bound (22),  $\sup_{t \leq \tau \leq t+h} |\tilde{b}_1(\tau) - \tilde{b}_2(\tau)|_E \leq L_i K_b |Y_1 - Y_2|_\infty$ , and  $\sup_{t \leq \tau \leq t+h} |\tilde{a}_1(\tau) - \tilde{a}_2(\tau)| \leq L_i K_a |Y_1 - Y_2|_\infty$ . With the upper bound (27), for  $t \leq \tau \leq t+h \leq T$  and for  $h \leq h_0$ ,

$$|r(\tau)|_E \leq L_i |Y_1 - Y_2|_\infty (K_b + K_a (C_1 h + |Y_2|_\infty (1 + C_1 h))) \leq C |Y_1 - Y_2|_\infty (1 + |Y_2|_\infty). \quad (28)$$

For a constant  $C$  only depending on  $h_0, K_a, K_b, L_i$  and  $C_1$ . We finally apply the Gronwall inequality (26). It yields  $|\delta(t+h)| \leq e^{L_i M_a h} (|y_{1,k} - y_{2,k}|_E + Ch |Y_1 - Y_2|_\infty (1 + |Y_2|_\infty)) \leq |Y_1 - Y_2|_\infty e^{L_i M_a h} (1 + Ch (1 + |Y_2|_\infty))$ , This implies the second stability condition (15) for  $h \leq h_0$ .

#### 4.3.2. Case of the EAB<sub>k</sub> scheme

Consider  $(t, h) \in \mathbb{R} \times \mathbb{R}^+$  and a vector  $Y = (y_1, \dots, y_k) \in E^k$ . Following the definition of the EAB<sub>k</sub> scheme given in section 2.1, we denote  $\bar{a} = a(t, y_k)$ ,  $g$  the function  $g(\tau, \xi) = b(\tau, \xi) + (a(\tau, \xi) - \bar{a})\xi = f(\tau, \xi) - \bar{a}\xi$  and  $\bar{g} = \bar{g}_{[t, Y, h]}$ . We have that  $\bar{g}$  is the Lagrange interpolation polynomial of  $g$ , specifically  $\bar{g} = \bar{g}_{[t, Y, h]}$ . The scheme generator is then given by the equation (25):  $s(t, Y, h) = z(t+h)$  with  $z' = \bar{a}z + \bar{g}$ , and  $z(t) = y_k$ . We first have the bound  $|\bar{a}| \leq M_a$ . As in the previous subsection,  $f$  being globally Lipschitz in  $y$ , one can find a constant  $R_f$  so that for  $0 \leq t \leq T$ ,  $|f(t, y)|_E \leq R_f(1 + |y|_E)$ . It follows that  $|g(\tau, \xi)|_E \leq R_f(|y|_E + 1) + M_a|y|_E \leq C_0/L_i(|y|_E + 1)$ , with  $C_0/L_i = R_f + M_a$ . Therefore, with the interpolation bound (21),  $\sup_{t \leq \tau \leq t+h} |\bar{g}(\tau)|_E \leq L_i \max_{0 \leq i \leq k-1} |g(t - ih, y_{k-i})|_E \leq C_0(|y|_E + 1)$ . By applying the Gronwall inequality (26), for  $0 \leq \tau \leq h$ ,  $|z(t + \tau)|_E \leq e^{M_a h} (|y_k|_E + hC(|Y|_\infty + 1))$ . Thus, there exists a constant  $C_1$  only depending on  $M_a$  and  $C_0$  such that, for  $0 \leq \tau \leq h$  and  $0 \leq h \leq h_0$ , the bound (27) holds. This gives the condition (14).

We now consider  $Y_1, Y_2 \in E^k$  for  $j = 1, 2$ , and denote as previously,  $\bar{a}_j = a(t, y_{j,k})$ ,  $g_j$  the function  $g_j(\tau, \xi) = f(\tau, \xi) - \bar{a}_j \xi$  and  $\bar{g}_j = \bar{g}_{[t, Y_j, h]}$ . With (25),  $|s(t, Y_1, h) - s(t, Y_2, h)|_E = |\delta(t+h)|$  with  $\delta = z_1 - z_2$  and with  $z_j$  given by,  $z_j' = \bar{a}_j z_j + \bar{g}_j$ , and  $z_j(t) = y_{j,k}$ . The function  $\delta$  satisfies the ODE,  $\delta' = \bar{a}_1 \delta + r(t)$ , with  $r(t) := (\bar{a}_1 - \bar{a}_2)z_2 + (\bar{g}_1 - \bar{g}_2)$ .

Now, we have,  $|g_1(\tau, y_{1,i}) - g_2(\tau, y_{2,i})|_E \leq |f(\tau, y_{1,i}) - f(\tau, y_{2,i})|_E + |\bar{a}_1| |y_{1,i} - y_{2,i}|_E + |\bar{a}_1 - \bar{a}_2| |y_{2,i}|_E \leq |Y_1 - Y_2|_\infty (K_f + M_a + K_a |Y_2|_\infty)$ . Thus, with the bound (22), for some  $C > 0$ ,  $\sup_{t \leq \tau \leq t+h} |\bar{g}_1(\tau) - \bar{g}_2(\tau)|_E \leq L_i \max_{0 \leq i \leq k-1} |g_1(t - ih, y_{1,k-i}) - g_2(t - ih, y_{2,k-i})|_E \leq C |Y_1 - Y_2|_\infty (1 + |Y_2|_\infty)$ .

Meanwhile we have the upper bound (27) that gives, for  $t \leq \tau \leq t+h \leq T$  and  $h \leq h_0$ ,  $|(\bar{a}_1 - \bar{a}_2)z_2|_E M_a |Y_1 - Y_2|_\infty |z_2(\tau)|_E \leq M_a |Y_1 - Y_2|_\infty (C_1 h + |Y_2|_\infty (1 + C_1 h))$ .

Altogether, we retrieve the upper bound (28) on  $r(t)$ . We can end the proof as for the I-EAB<sub>k</sub> case and conclude that the stability condition (15) holds for the EAB<sub>k</sub> scheme.

#### 4.4. Consistency

Consider a solution  $y \in C^1([0, T])$  to the problem (1). The functions  $a$  and  $b$  in (3) are assumed to be  $C^k$  regular so that  $y$  is  $C^{k+1}$  regular.

##### 4.4.1. Case of the EAB<sub>k</sub> scheme

The local error (18) for the EAB<sub>k</sub> scheme has been analyzed in [24]. The analysis remains valid for the case presented here and we only briefly recall it. The local error is obtained by subtracting (7) to (5).

$$|\varepsilon(t_n, h)|_E \leq \int_0^h e^{M_a(h-\tau)} |g_n(t + \tau, y(t + \tau)) - \bar{g}_n(t + \tau)|_E d\tau \leq h\varphi_1(M_a h) h^k \sup_{[0, T]} \left| \frac{d^k}{dt^k} (g_n(t, y(t))) \right|,$$

thanks to the interpolation error estimate (23). Finally, with the upper bound  $M_a$  on  $a_n$ , the last term can be bounded independently of  $n$ , for  $h \leq h_0$ .

##### 4.4.2. Case of the I-EAB<sub>k</sub> scheme

We denote  $\tilde{a} = \tilde{a}_{[t_n, Y(t_n), h]}$  and  $\tilde{b} = \tilde{b}_{[t_n, Y(t_n), h]}$ . The local error (18) for the I-EAB<sub>k</sub> scheme satisfies  $\varepsilon(t_n, h) = |\delta(t_{n+1})|_E$  with  $\delta = y - z$  and where  $z$  is defined by,  $z' = \tilde{a}z + \tilde{b}$ , and  $z(t_n) = y(t_n)$ , so that with (24) we have  $s(t_n, Y(t_n), h) = z(t_{n+1})$ . The function  $\delta$  is defined with  $\delta(t_n) = 0$  and  $\delta' = \tilde{a}\delta + r$ , with  $r(\tau) := (a(\tau, y(\tau)) - \tilde{a}(\tau))y(\tau) + (b(\tau, y(\tau)) - \tilde{b}(\tau))$ . The following constants only depend on the considered exact solution  $y$ , on the functions  $a$  and  $b$  in problem (3) and on  $T$ ,  $C_y = \sup_{[0, T]} |y|_E$ ,  $C_{a,y} = \sup_{[0, T]} \left| \frac{d^k}{dt^k} a(t, y(t)) \right|$ , and  $C_{b,y} = \sup_{[0, T]} \left| \frac{d^k}{dt^k} b(t, y(t)) \right|$ .

With the interpolation bound (23),  $|r(\tau)|_E \leq Ch^k$  on  $[t_n, t_{n+1}]$  with  $C = C_{a,y}C_y + C_{b,y}$ . It has already been showed in section 4.3 that  $\sup_{[t_n, t_{n+1}]} |\tilde{a}(\tau)| \leq L_i M_a$ . Therefore, with the Gronwall inequality (26),  $\varepsilon(t_n, h) = |\delta(t_{n+1})|_E \leq e^{L_i M_a h} hCh^k$ . Thus the EAB $_k$  scheme is consistent of order  $k$ .

## 5. Dahlquist stability

### 5.1. Background

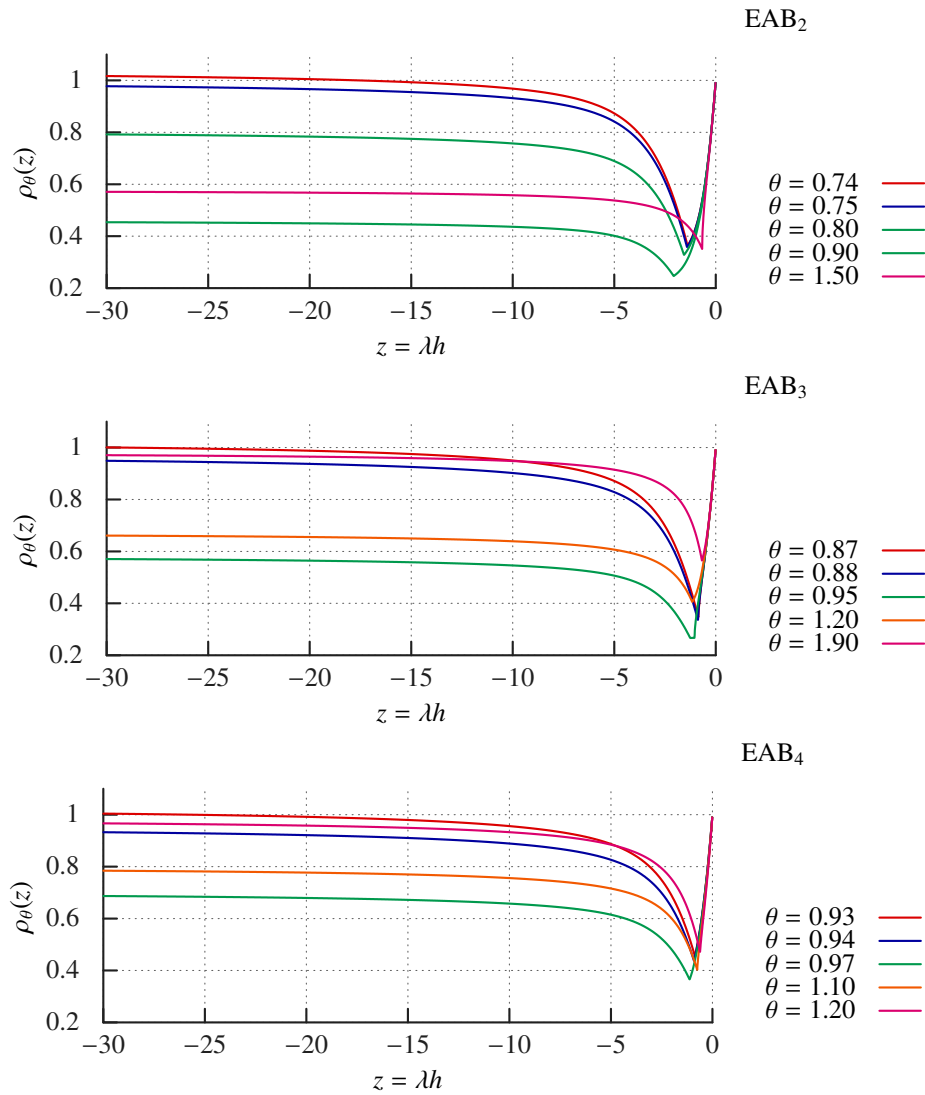


Figure 1: Stability function  $\rho_\theta(z)$  for  $z \in \mathbb{R}^-$ , for various values of  $\theta$  and for the three schemes EAB<sub>2</sub>, EAB<sub>3</sub> and EAB<sub>4</sub>.

The classical framework for the Dahlquist stability analysis is to set  $f(t, y)$  in problem (1) to  $f = \lambda y$ . For linear multistep methods, see e.g. [31], the numerical solutions satisfy  $|y_{n+1}/y_n| \leq \rho(\lambda h)$ , where  $\rho : \mathbb{C} \rightarrow \mathbb{R}^+$ . The function  $\rho$  is the stability function. It is defined point wise by the maximum root modulus of a family of polynomial depending on  $z = \lambda h$ . The stability domain is defined by  $D = \{z \in \mathbb{C}, \rho(z) < 1\}$ . The scheme is said to be:

- $A$  stable if  $\mathbb{C}^- \subset D$ ,
- $A(\alpha)$  stable if  $D$  contains the cone with axis  $\mathbb{R}^-$  and with half angle  $\alpha$ ,
- $A(0)$  stable if  $\mathbb{R}^- \subset D$ ,
- stiff stable if  $D$  contains a half plane  $\text{Re } z < x \in \mathbb{R}^-$ .

For exponential integrators, when setting  $a(t, y) = \lambda$  in the reformulation (3) of problem (1), the scheme is exact, and therefore also  $A$  stable. Such an equality does not hold in general. Then for exponential integrators the Dahlquist stability analysis has to incorporate the relationship between the stabilization term  $a(t, y)$  in (3) and the test function  $f = \lambda y$ . This is done here by considering the splitting,

$$f = \lambda y = ay + b, \quad a = \theta\lambda \quad \text{and} \quad b = \lambda(1 - \theta)y,$$

The parameter  $\theta > 0$  controls with what accuracy the exact linear part of  $f$  in equation 1 is captured by  $a$  in equation 3. In practice  $\theta \neq 1$ , though we may hope that  $\theta - 1$  is small. In this framework, the stability function and the stability domain depend on  $\theta$ , following the idea of Perego and Veneziani in [17]. For a fixed  $\theta$ , the stability function is  $\rho_\theta$  so that

$$\left| \frac{y_{n+1}}{y_n} \right| \leq \rho_\theta(\lambda h),$$

and the stability domain is  $D_\theta = \{z \in \mathbb{C}, \rho_\theta(z) < 1\}$ .

## 5.2. $A(0)$ stability

The stability functions  $\rho_\theta(z)$  are numerically studied for  $z \in \mathbb{R}^-$ . These functions have been plotted for different values of the parameter  $\theta$ . The results are depicted on figure 1. A limit  $\lim_{-\infty} |\rho_\theta|$  is always observed. The scheme is  $A(0)$  stable when this limit is lower than 1. From Figure 1,

- EAB<sub>2</sub> scheme is  $A(0)$  stable if  $\theta \geq 0.75$ ,
- EAB<sub>3</sub> scheme is  $A(0)$  stable if  $0.88 \leq \theta \leq 1.9$ ,
- EAB<sub>4</sub> scheme is  $A(0)$  stable if  $0.94 \leq \theta \leq 1.2$ .

Roughly speaking,  $A(0)$  stability holds for the EAB <sub>$k$</sub>  scheme if the exact linear part of  $f(t, y)$  in problem (1) is approximated with an accuracy of 75 %, 85 % or 95% for  $k = 2, 3$  or 4 respectively.

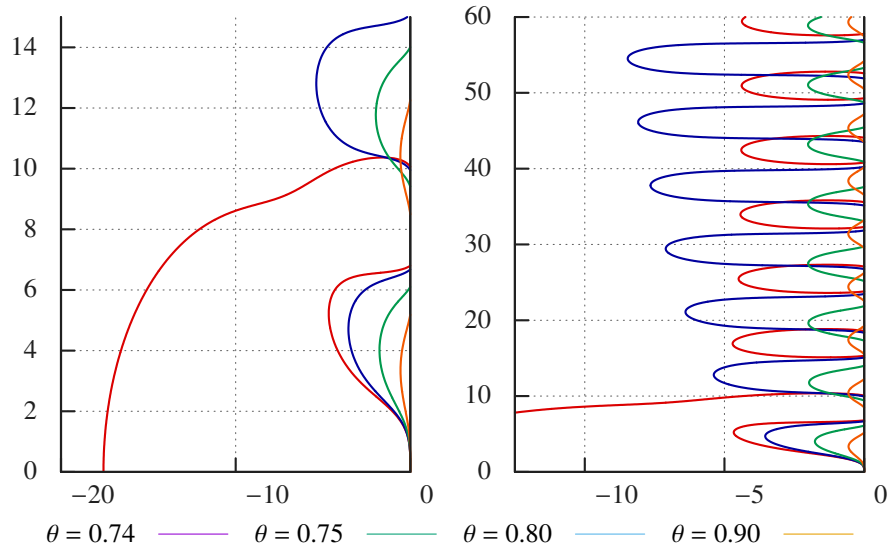


Figure 2: EAB<sub>2</sub>: isolines  $\rho_\theta(z) = 1$  for two different ranges. The stability domain  $D_\theta$  is on the left of the isoline.

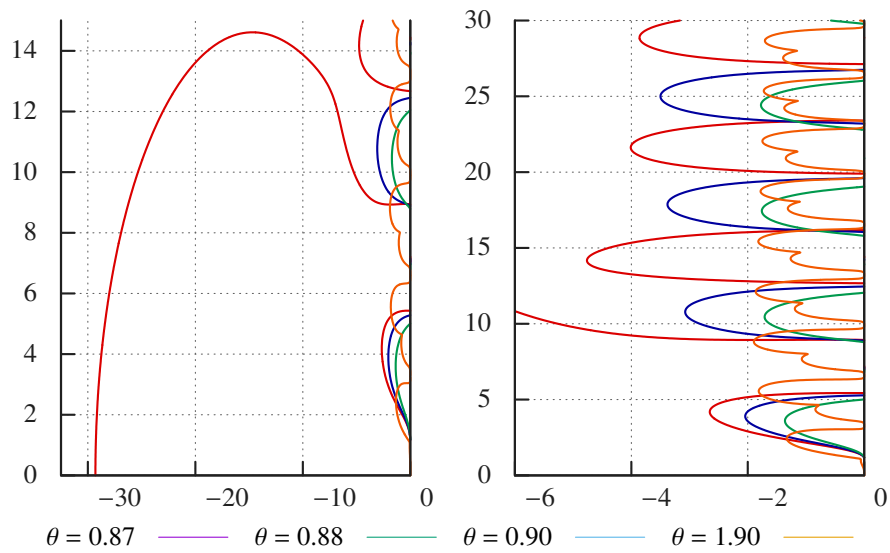


Figure 3: Same thing as figure 2 for the EAB<sub>3</sub> scheme.

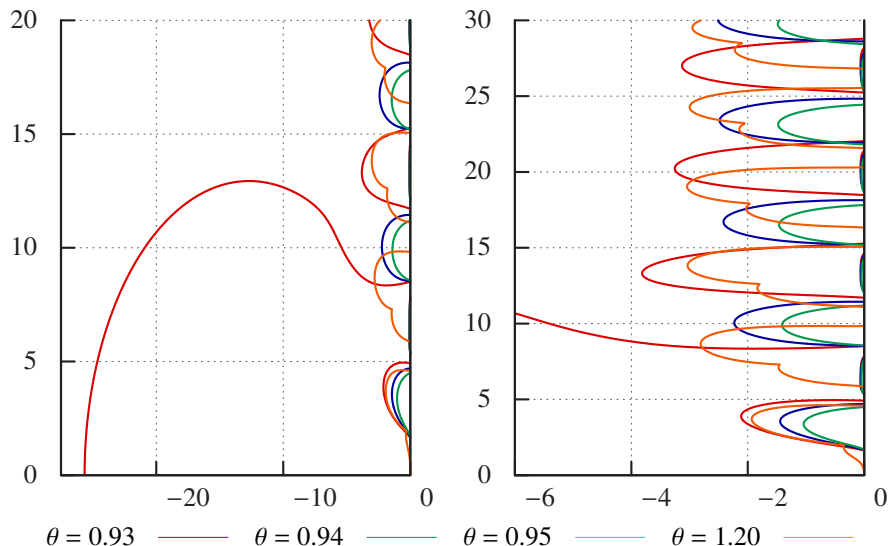


Figure 4: Same thing as figure 2 for the EAB<sub>4</sub> scheme.

### 5.3. $A(\alpha)$ stability

The stability domains  $D_\theta$  have been plotted for various values of  $\theta$  taken from figure 1. The results are depicted on the figures 2 to 4 for  $k = 2$  to 4 respectively. Each figure shows the isolines  $\rho_\theta(z) = 1$ . The stability domain  $D_\theta$  is on the left of these curves.

- Figure 2 shows that the EAB<sub>2</sub> scheme is  $A(\alpha)$  stable when  $\theta = 0.75, 0.8$  and  $0.9$  with  $\alpha \simeq 50, 60$  and  $80$  angle degrees respectively.
- Figure 3 displays  $A(\alpha)$  stability with  $\alpha \simeq 60, 70$  and  $60$  angle degrees for  $\theta = 0.88, 0.9$  and  $1.9$  respectively for the EAB<sub>3</sub> scheme.
- For the EAB<sub>4</sub> scheme eventually,  $A(\alpha)$  stability holds with an angle  $\alpha$  approximately of  $65, 70$  and  $60$  degrees for  $\theta = 0.94, 0.95$  and  $1.2$  respectively, as shown on figure 4.

In all cases, when  $A(\alpha)$  stability is observed, the unstable region inside  $\mathbb{C}^-$  is made of a discrete collection of uniformly bounded sets located along the imaginary axes. Hence, the stability domain  $D_\theta$  also contains half planes of the form  $\text{Re}(z) \leq a < 0$ . We conjecture that, when  $\theta$  is so that the EAB <sub>$k$</sub>  scheme is  $A(\alpha)$ -stable, then it is also stiff stable.

### 5.4. Conclusion

For explicit linear multistep methods,  $A(0)$  stability cannot occur, see [31, chapter V.2]. In contrast, EAB <sub>$k$</sub>  and I-EAB <sub>$k$</sub>  methods exhibit much better stability properties. When  $\theta$  is close enough to 1, they are  $A(\alpha)$  stable and stiff stable. Such stability properties are comparable with those of implicit linear multistep methods. In practice, these properties will hold if the stabilization term  $a(t, y)$  in (3) approximates the Jacobian of  $f(t, y)$  in (1) with an absolute discrepancy lower than 25 %, 10 % and 5 % for  $k = 2, 3$  and 4 respectively.

## 6. Numerical results

We present in this section numerical experiments that investigate the convergence, accuracy and stability properties of the I-EAB<sub>k</sub> and EAB<sub>k</sub> schemes. The membrane equation in cardiac electrophysiology is considered for two ionic models, the Beeler-Reuter (BR) and to the Ten-Tusscher *et al.* (TNNP) models. We refer to [4] and [6] for the definition of the models. The stiffness of these two models is due to the presence of different time scales ranging from 1 ms to 1 s, as depicted on figure 5. The stabilizer  $a_n$  always is a diagonal matrix in this section.

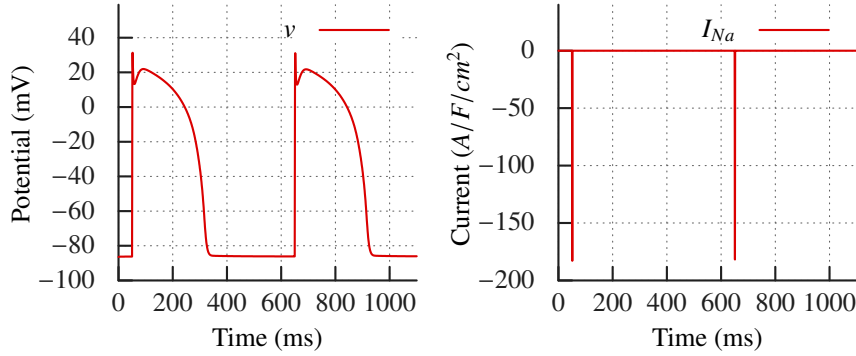


Figure 5: Two consecutive action potentials for the TNNP model: transmembrane potential  $v$  (left) and the fast sodium current  $I_{Na}$  (right), that is the main component of  $I_{ion}$  during the fast upstroke of the action potential.

The membrane equation has the general form, see [34, 4, 5, 6]:

$$\frac{dw_i}{dt} = \frac{w_{\infty,i}(v) - w_i}{\tau_i(v)}, \quad \frac{dc}{dt} = g(w, c, v), \quad \frac{dv}{dt} = -I_{ion}(w, c, v) + I_{st}(t), \quad (29)$$

where  $w = (w_1, \dots, w_p) \in \mathbb{R}^p$  is the vector of the gating variables,  $c \in \mathbb{R}^q$  is a vector of ionic concentrations or other state variables, and  $v \in \mathbb{R}$  is the cell membrane potential. These equations model the evolution of the transmembrane potential of a single cardiac cell. The four functions  $w_{\infty,i}(v)$ ,  $\tau_i(v)$ ,  $g(w, c, v)$  and  $I_{ion}(w, c, v)$  are given reaction terms. They characterize the cell model. The function  $I_{st}(t)$  is a source term. It represents a stimulation current.

The formulation (3) is recovered with,

$$a(t, y) = \begin{pmatrix} -1/\tau(v) & 0 & 0 \\ 0 & 0 & 0 \\ 0 & 0 & 0 \end{pmatrix}, \quad b(t, y) = \begin{pmatrix} w_{\infty}(v)/\tau(v) \\ g(y) \\ -I_{ion}(y) + I_{st}(t) \end{pmatrix},$$

for  $y = (w, c, v) \in \mathbb{R}^N$  (with  $N = p + q + 1$ ) and where  $-1/\tau(v) = \text{diag}(-1/\tau_i(v))_{i=1 \dots p}$ .

### 6.1. Implementation and computational cost

The computation of  $y_{n+1}$  with the I-EAB<sub>k</sub> and EAB<sub>k</sub> schemes requires the data  $y_{n-i}$ ,  $a_{n-i} := a(t_{n-i}, y_{n-i})$ , and  $b_{n-i} := b(t_{n-i}, y_{n-i})$  for  $i = 0 \dots k$ .



### *EAB<sub>k</sub> practical implementation*

Firstly, the  $g_{n-i} = b_{n-i} + (a_{n-i} - a_n)y_{n-i}$  are updated at each time step. Then the coefficients  $\gamma_{nj}$  in table 1 are computed. Secondly, the computation of  $y_{n+1}$  by formula (8) also requires the computation of the  $\varphi_j(a_n h)\gamma_{nj}$ . This is a matrix-vector product in general.

In the present case of a diagonal stabilizer, it becomes a scalar-scalar product per row. The  $\varphi_j(a_n h)$  are computed on all diagonal entries of  $a_n h$ . This computation simply necessitates to compute  $\varphi_0(a_n h) = e^{a_n h}$  (one exponential per non zero diagonal entry) thanks to the recursion rule (9).

In general, the relation (9) can be used to replace the computation of the  $\varphi_j(a_n h)\gamma_{nj}$  for  $j = 0 \dots k$  by the computation of a single product  $\varphi_k(a_n h)w_k$ . Denoting by  $w_1 = a_n y_n + b_n$  and  $w_j = \gamma_{nj} + a_n h w_{j-1}$ :

$$\begin{aligned} \text{EAB}_2 : y_{n+1} &= y_n + h(w_1 + \varphi_2(a_n h)w_2), \\ \text{EAB}_3 : y_{n+1} &= y_n + h(w_1 + w_2/2 + \varphi_3(a_n h)w_3), \\ \text{EAB}_4 : y_{n+1} &= y_n + h(w_1 + w_2/2 + w_3/6 + \varphi_4(a_n h)w_4). \end{aligned}$$

### *I-EAB<sub>k</sub> practical implementation*

In addition, the I-EAB<sub>k</sub> method (10) requires a quadrature rule of sufficient order to preserve the scheme accuracy and convergence order. We used the Simpson quadrature rule for the cases  $k = 2, 3$  and the three point Gaussian quadrature rule for  $k=4$ . We point out that  $a_n$  is assumed diagonal here so that the matrix exponentials below actually are scalar exponential.

The I-EAB<sub>k</sub> method with Simpson quadrature rule reads,

$$y_{n+1} = e^{\tilde{g}_1} (y_n + b_n h/6) + (\tilde{b}_1 + 4 e^\delta \tilde{b}_{1/2}) h/6,$$

where (with the notations of section 2.2)  $\tilde{g}_1 = \tilde{g}_n(t_{n+1})$ ,  $\delta = \tilde{g}_1 - \tilde{g}_n(t_n + h/2)$ ,  $\tilde{b}_1 = \tilde{b}_n(t_{n+1})$  and  $\tilde{b}_{1/2} = \tilde{b}_n(t_n + h/2)$ . These coefficients are given for  $k = 2$  by,

$$\tilde{g}_1 = (3a_n - a_{n-1})h/2, \quad \delta = (7a_n - 3a_{n-1})h/8, \quad \tilde{b}_1 = 2b_n - b_{n-1}, \quad \tilde{b}_{1/2} = (3b_n - b_{n-1})/2,$$

and for  $k = 3$  by,

$$\begin{aligned} \tilde{g}_1 &= (23a_n - 16a_{n-1} + 5a_{n-2})h/12, \quad \delta = (29a_n - 25a_{n-1} + 8a_{n-2})h/24, \\ \tilde{b}_1 &= 3b_n - 3b_{n-1} + b_{n-2}, \quad \tilde{b}_{1/2} = (15b_n - 10b_{n-1} + 3b_{n-2})/8. \end{aligned}$$

The I-EAB<sub>k</sub> method with the three point Gaussian quadrature rule reads,

$$y_{n+1} = e^{\tilde{g}_1} \left( y_n + \frac{h}{18} (5\tilde{b}_l e^{-\tilde{g}_l} + 8\tilde{b}_0 e^{-\tilde{g}_0} + 5\tilde{b}_r e^{-\tilde{g}_r}) \right),$$

with  $\tilde{b}_s = \tilde{b}_n(t_s)$ ,  $\tilde{g}_s = \tilde{g}_n(t_s)$  for  $s \in \{l, 0, r\}$  where  $t_l = t_n + (1 - \sqrt{3/5})h/2$ ,  $t_0 = t_n + h/2$ ,  $t_r = t_n + (1 + \sqrt{3/5})h/2$  and with  $\tilde{g}_1 = \tilde{g}_n(t_{n+1})$ . These parameters are linear combination of the data  $a_{n-i}, b_{n-i}$  for  $i = 0 \dots k-1$  with fixed coefficients. Formula for  $k = 4$  follow. The parameters  $\tilde{b}_s$  are given by

$$16\tilde{b}_0 = 35b_n - 35b_{n-1} + 21b_{n-2} - 5b_{n-3},$$

and

$$40\tilde{b}_r = (95 + 179\sqrt{15}/15)b_n - (107 + 119\sqrt{15}/5)b_{n-1} \\ + (69 + 79\sqrt{15}/5)b_{n-2} - (17 + 59\sqrt{15}/15)b_{n-3},$$

and  $\tilde{b}_l$  is the radical conjugate of  $\tilde{b}_r$  (the radical conjugate of  $x + \sqrt{y}$  is  $x - \sqrt{y}$ ). Finally, the parameters  $\tilde{g}_s$  definition is

$$24/h\tilde{g}_1 = 55a_n - 59a_{n-1} + 37a_{n-2} - 9a_{n-3}, \\ 384/h\tilde{g}_0 = 297a_n - 187a_{n-1} + 107a_{n-2} - 25a_{n-3},$$

and

$$200/h\tilde{g}_r = (797/4 + 45\sqrt{15})a_n - (2233/12 + 47\sqrt{15})a_{n-1} \\ + (1373/12 + 29\sqrt{15})a_{n-2} - (331/12 + 7\sqrt{15})a_{n-3},$$

and  $\tilde{g}_l$  is the radical conjugate of  $\tilde{g}_r$ .

### Computational cost

Consider an ODE system (1) whose numerical resolution cost is dominated by the computation of  $(t, y) \mapsto f(t, y)$ . This might be the case in general for “*large and complex models*”. For such problems explicit multistep methods are relevant since they will require one such operation per time step. In contrast, implicit methods, associated to a non linear solver, may necessitate a lot of these operations, especially for large time steps when convergence is harder to reach.

In addition, the I-EAB $_k$  and EAB $_k$  schemes need several specific operations. In the case of a diagonal function  $a(t, y)$  they have been previously described: the EAB $_k$  require one scalar exponential computation per non zero row of  $a(t, y)$ , the I-EAB $_k$  with Simpson rule needs twice more and the I-EAB $_3$  with 3 point Gaussian quadrature rule four times more. Such a cost is not negligible, but is at worst of same order than computing  $(t, y) \mapsto f(t, y)$  for complex models. For the TNNP model considered here, computing  $(t, y) \mapsto f(t, y)$  costs 50 scalar exponentials whereas the EAB $_k$  implementation adds 7 supplementary scalar exponentials per time step. In terms of cost per time step, the EAB $_k$  method is rather optimal. The relationship between accuracy and cost of the EAB $_k$  method has been investigated in [35]: more details are available in section 6.4.

### 6.2. Convergence

For the chosen application, no theoretical solution is available. Convergence properties are studied by computing a reference solution  $y_{ref}$  for a reference time step  $h_{ref}$  with the Runge Kutta 4 scheme. Numerical solutions  $y$  are computed to  $y_{ref}$  for coarsest time steps  $h = 2^p h_{ref}$  for increasing  $p$ . Any numerical solution  $y$  consists in successive values  $y_n$  at the time instants  $t_n = nh$ . On every interval  $(t_{3n}, t_{3n+3})$  the polynomial  $\bar{y}$  of degree at most 3 so that  $\bar{y}(t_{3n+i}) = y_{3n+i}$ ,  $i = 0 \dots 4$  is constructed. On  $(0, T)$ ,  $\bar{y}$  is a piecewise continuous polynomial of degree 3. Its values at the reference time instants  $nh_{ref}$  are computed. This provides a projection  $P(y)$  of the numerical solution  $y$  on the reference grid. Then  $P(y)$  can be compared with the reference solution  $y_{ref}$ . The numerical error is defined by,

$$e(h) = \frac{\max |v_{ref} - P(y)|}{\max |v_{ref}|}, \quad (30)$$

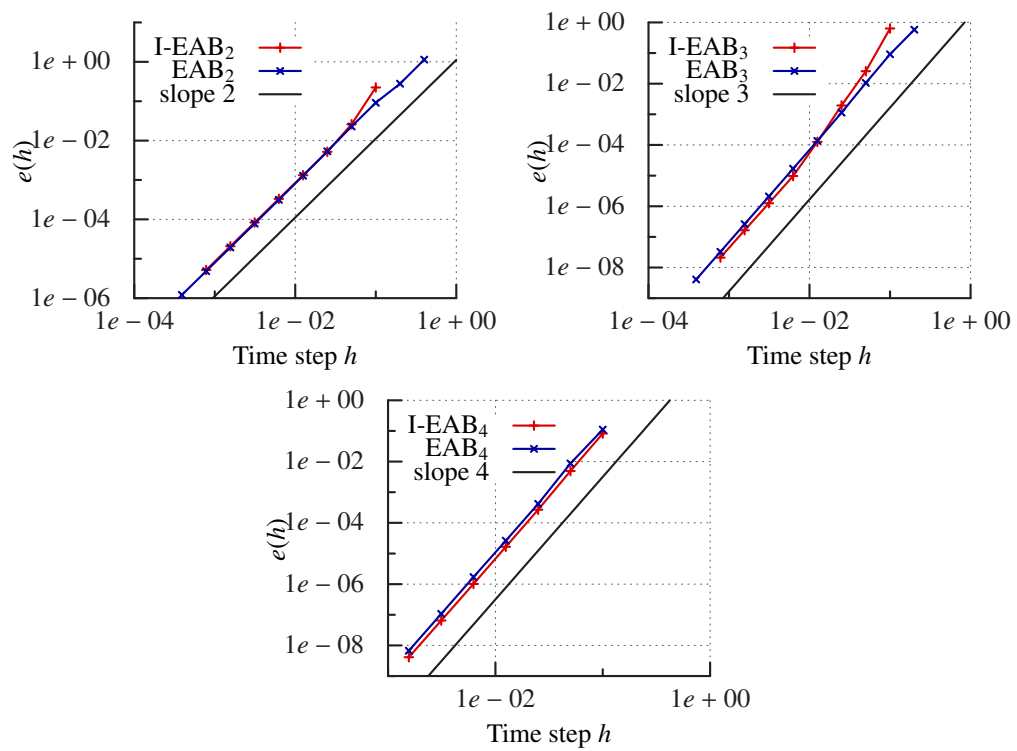


Figure 6: Relative  $L^\infty$  error  $e(h)$  for the I-EAB<sub>k</sub> and EAB<sub>k</sub> schemes,  $k = 2, 3$  and  $4$ , and for the BR model.

where the potential  $v$  is the last and stiffest component of  $y$  in equation 29.

The convergence graphs for the BR model are plotted on figure 6. All the schemes display the expected asymptotic behavior  $e(h) = O(h^k)$  as  $h \rightarrow 0$ , as proved in theorem 1.

### 6.3. Stability

The stiffness of the BR and TNNP models along one cellular electrical cycle (as depicted on figure 5) has been evaluated in [36]. The largest negative real part of the eigenvalues of the Jacobian matrix during this cycle is of  $-1170$  and  $-82$  for the TNNP and BR models respectively. This means that the TNNP model is 15 times stiffer than the BR model ( $15 \approx 1170/82$ ).

We want to evaluate the impact of this increase of stiffness in terms of stability for the  $EAB_k$  and  $I-EAB_k$  schemes and to provide a comparison with some other classical time stepping methods. To this aim we consider the *critical time step*  $\Delta t_0$ . It is defined as the largest time step such that the numerical simulation runs without overflow nor non linear solver failure for  $h < \Delta t_0$ . The numerical evaluation of  $\Delta t_0$  is easy for explicit methods. For implicit methods, the choice of the non linear solver certainly impacts  $\Delta t_0$ . Without considering more deeply this problem, we just carefully set up the non linear solver, so as to provide the largest  $\Delta t_0$ . In practice, we have been using a Jacobian free Krylov Newton method.

Table 2: Critical time step  $\Delta t_0$

	(a) Classical methods		(b) I-EAB <sub>k</sub> and EAB <sub>k</sub> exponential methods		
	BR	TNNP		BR	TNNP
AB <sub>2</sub>	$0.124 \times 10^{-1}$	$0.850 \times 10^{-3}$	I-EAB <sub>2</sub>	0.121	0.103
BDF <sub>2</sub>	0.306	0.158	EAB <sub>2</sub>	0.424	0.233
AB <sub>3</sub>	$0.679 \times 10^{-2}$	$0.464 \times 10^{-3}$	I-EAB <sub>3</sub>	0.103	0.123
BDF <sub>3</sub>	0.362	0.181	EAB <sub>3</sub>	0.203	0.108
AB <sub>4</sub>	$0.372 \times 10^{-2}$	$0.255 \times 10^{-3}$	I-EAB <sub>4</sub>	0.133	0.106
RK <sub>4</sub>	$0.338 \times 10^{-1}$	$0.255 \times 10^{-2}$	EAB <sub>4</sub>	0.122	$0.756 \times 10^{-1}$
BDF <sub>4</sub>	0.423	0.201			

Results are on table 2. The Adams Bashforth (AB<sub>k</sub>) and the backward differentiation (BDF<sub>k</sub>) methods of order  $k$  have been considered, together with the RK<sub>4</sub> scheme.

The AB<sub>k</sub> and the RK<sub>4</sub> schemes have bounded stability domain (see [31, p. 243]). Then it is expected for the critical time step to be divided by a factor close to 15 between the BR and TNNP models. Results presented in table 2 show this behavior.

The BDF<sub>2</sub> scheme is  $A$ -stable whereas the BDF<sub>3</sub> and BDF<sub>4</sub> are  $A(\alpha)$ -stable with large angle  $\alpha$  (see [31, p. 246]). Hence the critical time step is expected to remain unchanged between the two models. Table 2 shows that the  $\Delta t_0$  actually are divided by approximately 2.

The critical time steps for the I-EAB<sub>k</sub> and EAB<sub>k</sub> models are presented in table 2. The critical time steps for the I-EAB<sub>k</sub> schemes remain almost unchanged from the BR to the TNNP model. For the EAB<sub>k</sub>, they are divided by approximately 2, which behavior is similar as for the BDF<sub>k</sub> method.

As a conclusion, for the present application, the EAB<sub>k</sub> and I-EAB<sub>k</sub> methods are as robust to stiffness than the implicit BDF<sub>k</sub> schemes, though being explicit. As a matter of fact, section 5 shows that the stability domains for the I-EAB<sub>k</sub> and EAB<sub>k</sub> schemes depend on the discrepancy

between the complete Jacobian matrix and  $a(t, y)$ . In the present case,  $a(t, y)$  only contains a part of the Jacobian matrix diagonal. It is very interesting to notice that robustness to stiffness is actually achieved with this choice. It is finally also interesting to see that the critical time steps of implicit and exponential methods are of the same order.

#### 6.4. Accuracy

In terms of accuracy, the schemes can be compared using the relative error  $e(h)$  in equation (30). The  $EAB_k$  and  $I-EAB_k$  schemes can be compared with the  $AB_k$  methods only at very small

Table 3: Accuracy  $e(h)$  for the  $AB_k, I-EAB_k$  and  $EAB_k$  schemes: using the BR model and fixed time step  $h = 10^{-3}$

	$k = 2$	$k = 3$	$k = 4$
$AB_k$	$5.32 \times 10^{-6}$	$4.33 \times 10^{-8}$	$8.69 \times 10^{-10}$
$I-EAB_k$	$8.55 \times 10^{-6}$	$4.44 \times 10^{-8}$	$7.30 \times 10^{-10}$
$EAB_k$	$7.90 \times 10^{-6}$	$7.00 \times 10^{-8}$	$1.16 \times 10^{-9}$

time steps, because of the lack of stability of  $AB_k$  schemes (see table 2). In table 6.4 are given the accuracies of these methods for a given time step  $h = 10^{-3}$  and for the BR model. It is observed that the same level of accuracy is obtained with  $AB_k$  and  $EAB_k$  at fixed  $k$ . These figures illustrate that inside the asymptotic convergence region,  $EAB_k, I-EAB_k$  and  $AB_k$  schemes are equivalent in terms of accuracy.

Table 4: Accuracy for the TNNP model

(a) $EAB_k$			
$h$	$k = 2$	$k = 3$	$k = 4$
0.1	0.351	0.530	
0.05	$9.01 \times 10^{-2}$	$5.59 \times 10^{-2}$	$8.93 \times 10^{-2}$
0.025	$2.14 \times 10^{-2}$	$7.34 \times 10^{-3}$	$8.34 \times 10^{-3}$
(b) $BDF_k$			
$h$	$k = 2$	$k = 3$	$k = 4$
0.1			0.129
0.05	$3.57 \times 10^{-2}$	$1.15 \times 10^{-2}$	$1.44 \times 10^{-2}$
0.025	$1.10 \times 10^{-2}$	$2.58 \times 10^{-3}$	$2.38 \times 10^{-3}$

Comparison at large time steps between the  $EAB_k$  and  $BDF_k$  for the TNNP model is shown in table 4. These figures show that for large time steps  $BDF_k$  is more accurate than  $EAB_k$ . A gain in accuracy of factor 2.5, 5 and 6 is observed for  $h = 0.05$  and for  $k=2, 3$  and 4 respectively. However, compare row 3 for  $EAB_k$  ( $h = 0.025$ ) with row 2 for  $BDF_k$  ( $h = 0.05$ ). It shows that the numerical solutions with an accuracy close to 0.01 are obtained when dividing the time step by (at most) 2 between  $BDF_k$  and  $EAB_k$ . Meanwhile,  $EAB_k$  with  $h = 0.025$  costs less than  $BDF_k$  with  $h = 0.05$ , as developed in section 6.1.

We conclude that  $EAB_k$  schemes provide a cheaper way to compute numerical solutions at large time step for a given accuracy. The same conclusion also holds for the BR model, see table

5. A deeper analysis of the relationship between accuracy and computational cost for the  $EAB_k$  scheme as compared to other methods is available in [35] with the same conclusion.

Table 5: Accuracy for the BR model

(a) $EAB_k$			
$h$	$k = 2$	$k = 3$	$k = 4$
0.2	0.284	0.516	
0.1	$9.26 \times 10^{-2}$	$9.17 \times 10^{-2}$	0.119
0.05	$8.20 \times 10^{-2}$	$1.09 \times 10^{-2}$	$8.96 \times 10^{-3}$
(b) $BDF_k$			
$h$	$k = 2$	$k = 3$	$k = 4$
0.2	$9.74 \times 10^{-2}$	$4.09 \times 10^{-2}$	$4.98 \times 10^{-2}$
0.1	$3.44 \times 10^{-2}$	$1.04 \times 10^{-2}$	$1.27 \times 10^{-2}$
0.05	$9.74 \times 10^{-3}$	$2.29 \times 10^{-3}$	$2.02 \times 10^{-3}$

In table 5 are given the accuracies at large time step now considering the BR model. Comparison with table 4 shows that accuracy is preserved by dividing  $h$  by 2 when switching from the BR to the TNNP model. As already said, the TNNP model is 15 times stiffer than the BR model.

We conclude that the  $EAB_k$  schemes also exhibit a large robustness to stiffness in terms of accuracy. This robustness is equivalent as for the implicit  $BDF_k$  schemes. This is remarkable for an explicit scheme, as for the robustness to stiffness in terms of critical time step discussed in the previous subsection.

## 7. Acknowledgments

This study received financial support from the French Government as part of the “Investissement d’avenir” program managed by the National Research Agency (ANR), Grant reference ANR-10-IAHU-04. It also received fundings of the project ANR-13-MONU-0004-04.

- [1] J. Clements, J. Nenonen, P. Li, B. Horacek, Activation dynamics in anisotropic cardiac tissue via decoupling, *Ann. Biomed. Eng.* 32 (7) (2004) 984–990.
- [2] P. Colli-Franzone, L. Pavarino, B. Taccardi, Monodomain simulations of excitation and recovery in cardiac blocks with intramural heterogeneity, in: A. F. Frangi, P. I. Radeva, A. Santos, M. Hernandez (Eds.), *Functional Imaging and Modeling of the Heart*, Vol. 3504 of *Theoretical Computer Science and General Issues*, Springer-Verlag Berlin Heidelberg, 2005, pp. 267–277.
- [3] P. C. Franzone, L. Pavarino, B. Taccardi, Simulating patterns of excitation, repolarization and action potential duration with cardiac bidomain and monodomain models, *Mathematical Biosciences* 197 (1) (2005) 35 – 66.
- [4] G. W. Beeler, H. Reuter, Reconstruction of the action potential of ventricular myocardial fibres, *J. Physiol.* 268 (1) (1977) 177–210.
- [5] C. H. Luo, Y. Rudy, A dynamic model of the cardiac ventricular action potential. I. Simulations of ionic currents and concentration changes., *Circ. Res.* 74 (6) (1994) 1071–1096.
- [6] K. H. W. J. ten Tusscher, D. Noble, P. J. Noble, A. V. Panfilov, A model for human ventricular tissue, *Am. J. Physiol. Heart Circ. Physiol.* 286 (4) (2004) H1573–H1589.
- [7] V. Iyer, R. Mazhari, R. L. Winslow, A computational model of the human left-ventricular epicardial myocyte, *Biophys. J.* 87 (3) (2004) 1507–1525.
- [8] M. Hochbruck, C. Lubich, H. Selhofer, Exponential integrators for large systems of differential equations, *SIAM J. Sci. Comput.* 19 (5) (1998) 1552–1574.

- [9] S. M. Cox, P. C. Matthews, Exponential time differencing for stiff systems, *J. Comput. Phys.* 176 (2) (2002) 430–455.
- [10] M. Hochbruck, A. Ostermann, Explicit exponential Runge-Kutta methods for semilinear parabolic problems, *SIAM J. Numer. Anal.* 43 (3) (2005) 1069–1090.
- [11] M. Hochbruck, A. Ostermann, J. Schweitzer, Exponential Rosenbrock-type methods, *SIAM J. Numer. Anal.* 47 (1) (2009) 786–803.
- [12] M. Tokman, J. Loffeld, P. Tranquilli, New adaptive exponential propagation iterative methods of Runge-Kutta type, *SIAM J. Sci. Comput.* 34 (5) (2012) A2650–A2669.
- [13] V. T. Luan, A. Ostermann, Explicit exponential Runge-Kutta methods of high order for parabolic problems, *J. Comput. Appl. Math.* 256 (2014) 168–179.
- [14] B. Minchev, W. M. Wright, A review of exponential integrators for first order semi-linear problems, Preprint Numerics 2/2005, Norges Teknisk-Naturvitenskapelige Universitet (2005).
- [15] M. Hochbruck, A. Ostermann, Exponential integrators, *Acta Numer.* 19 (2010) 209–286.
- [16] M. Hochbruck, A short course on exponential integrators, in: Z. Bai, W. Gao, Y. Su (Eds.), *Matrix Functions and Matrix Equations*, Vol. 19 of *Contemp. Appl. Math.*, Higher Ed. Press, Beijing, 2015, pp. 28–49.
- [17] M. Perego, A. Veneziani, An efficient generalization of the Rush-Larsen method for solving electro-physiology membrane equations, *ETNA* 35 (2009) 234–256.
- [18] C. Börgers, A. R. Nectow, Exponential time differencing for Hodgkin-Huxley-like ODEs, *SIAM J. Sci. Comput.* 35 (3) (2013) B623–B643.
- [19] J. Certaine, The solution of ordinary differential equations with large time constants, in: A. Ralston, H. S. Wilf (Eds.), *Mathematical Methods for Digital Computers*, John Wiley & Sons, 1960, pp. 128–132.
- [20] S. P. Nørsett, An A-stable modification of the Adams-Bashforth methods, in: J. L. Morris (Ed.), *Conference on the Numerical Solution of Differential Equations: Held in Dundee/Scotland, June 23–27, 1969*, Springer, Berlin, Heidelberg, 1969, pp. 214–219.
- [21] M. Tokman, Efficient integration of large stiff systems of ODEs with exponential propagation iterative (EPI) methods, *J. Comput. Phys.* 213 (2) (2006) 748–776.
- [22] M. P. Calvo, C. Palencia, A class of explicit multistep exponential integrators for semilinear problems, *Numer. Math.* 102 (3) (2006) 367–381.
- [23] A. Ostermann, M. Thalhammer, W. M. Wright, A class of explicit exponential general linear methods, *BIT* 46 (2) (2006) 409–431.
- [24] M. Hochbruck, A. Ostermann, Exponential multistep methods of Adams-type, *BIT* 51 (4) (2011) 889–908.
- [25] W. Auzinger, M. Lapińska, Convergence of rational multistep methods of Adams-Padé type, Tech. rep., ASC Report, Vienna University of Technology (2011).
- [26] A. Koskela, A. Ostermann, Exponential Taylor methods: analysis and implementation, *Comput. & Math. with Appl.* 65 (3) (2013) 487–499.
- [27] D. Lee, S. Preiser, A class of non linear multistep A-stable numerical methods for solving stiff differential equations, *Comput. & Math with Appl.* 4 (1978) 43–51.
- [28] M. T. Chu, An automatic multistep method for solving stiff initial value problems, *J. Comput. Appl. Math.* 9 (3) (1983) 229–238.
- [29] P. Tranquilli, A. Sandu, Rosenbrock-Krylov methods for large systems of differential equations, *SIAM J. Sci. Comput.* 36 (3) (2014) A1313–A1338.
- [30] G. Rainwater, M. Tokman, A new class of split exponential propagation iterative methods of Runge-Kutta type (sEPIRK) for semilinear systems of ODEs, *J. Comput. Phys.* 269 (2014) 40–60.
- [31] E. Hairer, G. Wanner, *Solving Ordinary Differential Equations II*, Vol. 14 of *Springer Series in Computational Mathematics*, Springer, Berlin, Heidelberg, 1996.
- [32] E. Hairer, S. P. Nørsett, G. Wanner, *Solving Ordinary Differential Equations I*, Vol. 8 of *Springer Series in Computational Mathematics*, Springer-Verlag, Berlin, 1993.
- [33] S. S. Dragomir, *Some Gronwall type inequalities and applications*, Nova Science Publishers, Inc., Hauppauge, New York, 2003.
- [34] A. Hodgkin, A. Huxley, A quantitative description of membrane current and its application to conduction and excitation in nerve, *J. Physiol.* 117 (1952) 500–544.
- [35] C. Douanla Lontsi, Y. Coudière, C. Pierre, Efficient high order schemes for stiff ODEs in cardiac electrophysiology, in: M. Lo, E. Badouel, N. Gmati (Eds.), *Proceedings of CARI 2016, Hammamet, Tunisia, 2016*, pp. 312–319.
- [36] R. J. Spiteri, C. D. Ryan, Stiffness analysis of cardiac electrophysiological models, *Ann. Biomed. Eng.* 38 (2010) 3592–3604.